Merged interaction regions at 1 AU

L. Burlaga,[1] D. Berdichevsky,[2] N. Gopalswamy,[1] R. Lepping,[1] and T. Zurbuchen[3]

Received 16 June 2003; revised 5 August 2003; accepted 26 September 2003; published 9 December 2003.

[1] We discuss the existence of large, complex merged interaction regions (MIRs) in the solar wind near Earth. MIRs can have configurations that cause more prolonged geomagnetic effects than a single flow structure. A MIR or successive MIRs can produce relatively long lasting Forbush decreases at 1 AU. We illustrate MIRs at 1 AU with two examples (MIR-1 and MIR-2) seen by WIND and ACE in the interval from 18 March through 29 March 2002. We determined the probable structure and origin of each in terms of interacting flows and shocks using in situ and solar observations, but we emphasize that there are uncertainties that cannot be resolved with these data alone. The MIRs were relatively large structures with radial extent ≈2/3 and 3/4 AU, respectively. MIR-1 was formed by interactions related to at least two complex ejecta, a magnetic cloud, and two shocks. MIR-2 was related to a corotating stream, the heliospheric plasma sheet (HPS), two complex ejecta, a magnetic cloud and at least two shocks. A MIR can evolve significantly while it moves to 1 AU, and memory of the conditions near the Sun is lost in the process. Thus one cannot unambiguously determine the structure of a MIR and the manner in which it formed using observations from a single spacecraft at 1 AU. The magnetic field strength profiles in MIRs are not correlated with the speed and density profiles so that one cannot infer the magnetic field strength in MIRs from remote sensing observation that give density and speed information. It will be possible to better understand the dynamical processes leading to the formation of MIRs with remote sensing observations, but they cannot measure the magnetic fields in MIRs. *INDEX TERMS:* 2111 Interplanetary Physics: Ejecta, driver gases, and magnetic clouds; 2134 Interplanetary Physics: Interplanetary magnetic fields; 2164 Interplanetary Physics: Solar wind plasma; 2139 Interplanetary Physics: Interplanetary shocks; 2104 Interplanetary Physics: Cosmic rays; *KEYWORDS:* merged interaction regions, magnetic field, shocks, composition, ejecta, magnetic clouds

Citation: Burlaga, L., D. Berdichevsky, N. Gopalswamy, R. Lepping, and T. Zurbuchen, Merged interaction regions at 1 AU, *J. Geophys. Res.*, *108*(A12), 1425, doi:10.1029/2003JA010088, 2003.

1. Introduction

[2] Interactions among flows between the Sun and 1 AU can produce "merged interaction regions" (MIRs) with strong magnetic fields at 1 AU. MIRs can strongly influence geomagnetic and ionospheric activity, cosmic ray modulation, and energetic particle propagation. In situ observations of the solar wind at a point at 1 AU provide signals giving detailed information about the local structure of a MIR moving past that point, but the signals cannot tell us directly how the MIR formed. Continuous remote sensing observations (such as the available scintillation observations and the observations that will be obtained by the STEREO spacecraft) together with solar observations can provide a global view of the speed and density patterns related to the flows and interactions that produce the MIRs. Unfortunately, the remote sensing observations cannot provide detailed information about the structures, and they give no information about the magnetic fields within MIRs, which are crucial in SEC (Sun-Earth Connection) processes. A fundamental problem in Sun-Earth Connections is to predict the plasma and magnetic field profiles at a point at 1 AU, given the appropriate solar observations. The problem of predicting the profiles in MIRs at 1 AU is important and particularly challenging.

[3] Interaction regions are defined as regions in which the sum of the magnetic field and plasma pressure is relatively high [*Burlaga and Ogilvie*, 1970]. Several types of interaction regions are found at 1 AU: corotating interaction regions ahead of corotating streams (CRS), interaction regions ahead of ejecta, and interaction regions in the sheaths behind transient shocks. In practice, interaction regions can usually be identified by magnetic field observations alone, since interaction regions have a scale of the order of 12 hours or more and the magnetic and plasma pressures are generally positively correlated on these scales [*Burlaga and Ogilvie*, 1970]. Since the magnetic field strength is high in magnetic clouds and in some other types

[1]Laboratory for Extraterrestrial Physics, NASA Goddard Space Flight Center, Greenbelt, Maryland, USA.
[2]L-3 Communications, EER Systems, Inc., Largo, Maryland, USA.
[3]Space Research Laboratory, University of Michigan, Ann Arbor, Michigan, USA.

0148-0227/03/2003JA010088

of ejecta, interaction regions might include ejecta themselves. We consider two types of ejecta: (1) magnetic clouds defined by *Burlaga et al.* [1981] and (2) complex ejecta (CE) that include all types of ejecta that are not magnetic clouds [*Burlaga et al.*, 2001, 2002]. Early work on ejecta is reviewed by *Hundhausen* [1972, 1999], *Burlaga* [1995], and *Gosling* [1996, 1997]. See also *Cane et al.* [2000] and *Cane and Richardson* [2003].

[4] Merged interaction regions form by the interaction and coalescence of individual interaction regions and ejecta [*Burlaga*, 1995, chapter 8]. Neighboring corotating interaction regions interact as one fast corotating stream overtakes the slower corotating stream. A transient shock can interact with a corotating interaction region. A corotating shock can interact with a magnetic cloud. Ejecta can interact with other ejecta, and so on. Much is known about the formation of MIRs beyond 1 AU because one can (1) compare in situ observations of flows and interaction regions 1 AU with those at larger distances and (2) model the evolution of flows and interaction regions with observations at 1 AU as input. However, relatively little is known about the structure and formation MIRs observed at $\leq$1AU.

[5] The Helios spacecraft provided an opportunity to study flows and shocks between 0.3 AU and 1 AU [*Schwenn*, 1991] and their interactions [*Behannon et al.*, 1991; *Burlaga et al.*, 1983, 1985a, 1987; *Burlaga*, 1995]. Observations of coronal mass ejections by the LASCO instrument [*Brueckner et al.*, 1995] on SOHO were used to show that CMEs interact and merge to produce fast streams and complex ejecta at 1 AU [*Burlaga et al.*, 2001, 2002]. *Berdichevsky et al.* [1998, 2003] and *Lepping et al.* [2001] also analyzed the coalescence of ejecta. *Gopalswamy et al.* [2001] used observations of CMEs by LASCO and observations of radio waves by WIND to show that CMEs can interact with one another even in the solar corona.

[6] This paper discusses the challenges of understanding and predicting the magnetic fields in MIRs at 1 AU. We analyze two MIRs observed at 1 AU during March 2002 that illustrate the basic features of MIRs at 1 AU. By combining the detailed in situ plasma and magnetic field observations made by one spacecraft near 1 AU with solar observations of photospheric magnetic fields, coronal holes, and coronal mass ejections, we derive a qualitative picture of the structure, formation, and evolution of these two MIRs. We point out the limitations of these results and show how a more complete (but still limited) understanding of formation of MIRs at 1 AU could be obtained by the addition of continuous remote sensing observations from STEREO, SMEI [*Jackson and Hick*, 2002], and interplanetary scintillation (IPS) observations.

2. Overview of the Solar Wind and Solar Observations

[7] Two large-scale features of the interplanetary medium that are observed throughout most of the solar cycle are the heliospheric current sheet and corotating streams. Since these two features generally persist longer than the time it takes for the ejecta to move from the Sun to Earth, they determine the basic structure of the medium through which ejecta move. The intersection of the heliospheric current sheet with a source surface near the Sun forms a curve (the "neutral line") that is the boundary between positive magnetic fields in one hemisphere and negative magnetic fields in the other. Corotating streams originate from coronal holes, which are regions of open magnetic lines on the Sun. Given observations of the photospheric magnetic field in the Sun, it is possible to predict the locations of the coronal holes and other regions with open magnetic fields as well as the neutral line, using a potential field model and a source surface [*Schatten et al.*, 1969; *Altschuler and Newkirk*, 1969; *Sheeley and Wang*, 1991]. It was found by *Wang et al.* [1997] and *Wang and Sheeley* [1997] that one could predict the speed in corotating streams by determining the spreading of the magnetic field lines from coronal holes, using the potential field model between the photosphere and 2.5 solar radii. Maps of these features as a function of Carrington longitude and the heliospheric latitude are computed routinely and posted by NOAA/SEC on http://solar.sec.noaa.gov/ws/index.html. Figure 1 shows a part of such a map, based on magnetic field observations from the Wilcox Solar Observatory (WSO), for the period considered in this paper. *Hundhausen* [1977] reviewed the relations between the solar wind observations and solar observations such as those in Figure 1. Recent work concerning the mapping of corotating streams to open field lines on the Sun was published by *Neugebauer et al.* [2002] and *Neugebauer and Liewer* [2003].

[8] The top panel in Figure 1 shows a map of the regions of open magnetic field lines, corresponding to coronal holes, as a function of Carrington longitude and heliographic latitude. The coronal holes are colored according to the solar wind speed that is computed from the divergence from these coronal holes. We shall analyze solar wind data from the WIND and ACE spacecraft located within $\pm 7.5^\circ$ of the equatorial plane of the Sun. The numbers at the top of the panel are the dates of central meridian passage of the points marked by plus signs in the middle of each of the panels in Figure 1. Two coronal holes crossed the equatorial plane on Carrington rotation 1987. The first coronal hole (CH-1) was located near Carrington longitude 145°, and it passed central meridian on 18 March 2002. The second coronal hole (CH-2) was located near Carrington longitude 85°, and it passed central meridian on 23 March 2002.

[9] The middle panel of Figure 1 shows a curve corresponding to a neutral line on a source surface, which is determined by extrapolating photospheric fields using a potential field model. The neutral line is the locus of the heliospheric current sheet (HCS) at the model source surface. The HCS crosses the solar equatorial plane at a relatively large angle at a longitude between the longitudes of CH-1 and CH-2. Thus a sector boundary (SB) at which the polarity of the magnetic field reverses should be observed in the solar wind near the ecliptic plane.

[10] The bottom panel of Figure 1 shows a map of the solar wind speed projected on the Sun as a function of latitude and Carrington longitude. This figure shows a narrow band of slow solar wind above the magnetic neutral line. The estimated solar wind speed near Earth as a function of time is given approximately by the colors on the line of 0° heliospheric latitude, moving from right to left in Figure 1.

[11] The predicted speed profile, V(t), at 1 AU upstream of the Earth, based on the potential field model and the solar

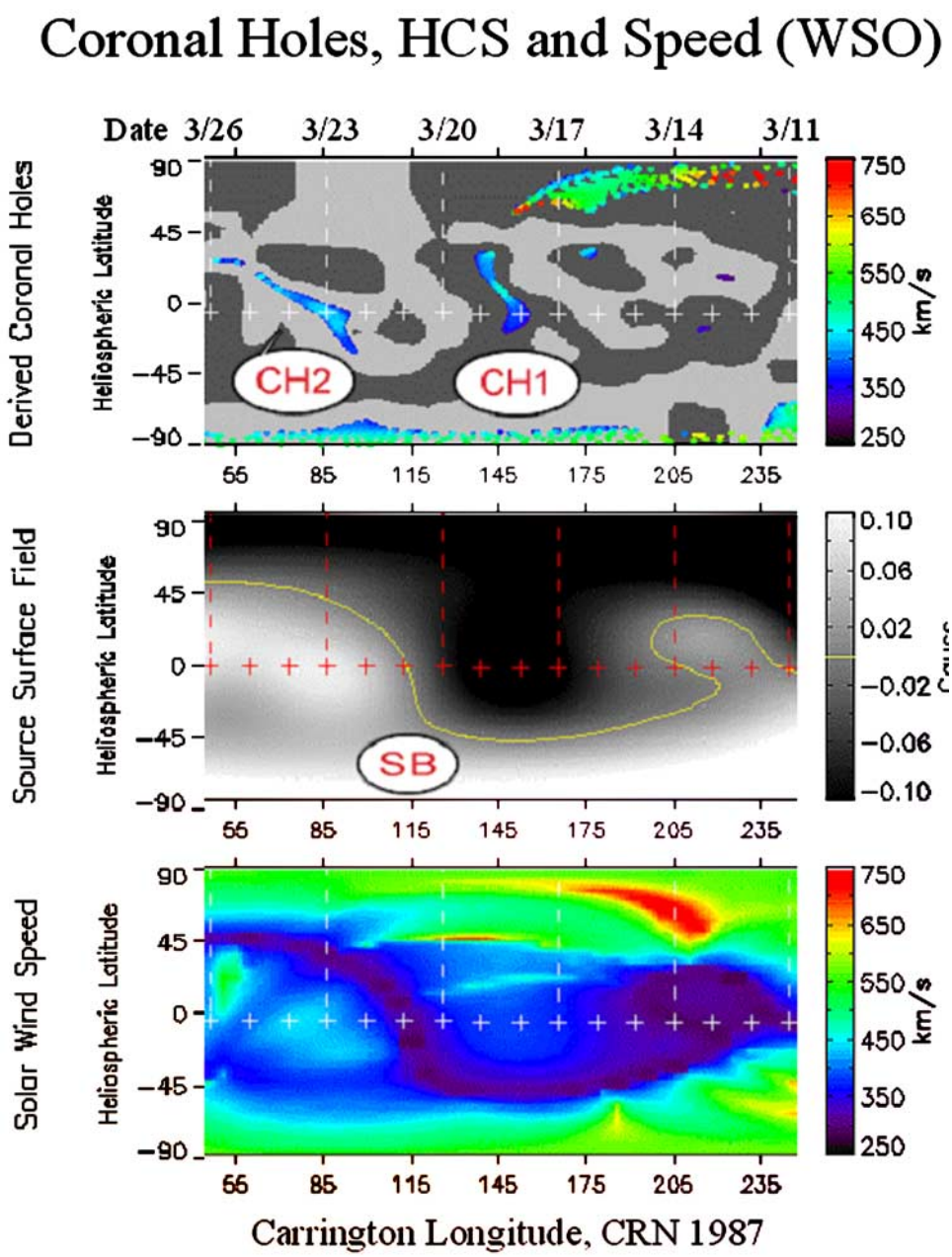

Figure 1. (top) Two coronal holes on Carrington rotation 1987 derived from solar magnetic field observations and the potential field model. (middle) The magnetic neutral line (yellow) separating positive and negative polarities of the solar magnetic field. (bottom) The solar wind speed on Carrington rotation 1987.

observations in Figure 1, is simple: two corotating streams separated by a slow flow. Assuming that the mean propagation time of the solar wind from the Sun to 1 AU was 4 days, corresponding to 430 km/s, Figure 1 predicts that ACE and WIND should have observed the following flow pattern, with an uncertainty of ≈±1 day: (1) a corotating stream from CH-1 with the speed of ≈400 km/s centered on ≈22 March (81), (2) a slow flow (≈300 km/sec) near 24 March (83), and (3) a corotating stream from CH-2 with the speed of V ≈ 450 km/sec centered on 27 March (86). Throughout this paper the number in parenthesis following a date is the time in DOY (1 January = 1), which is used in the plots of particle and magnetic field data.

[12] The observed speed profile at 1 AU, shown in Figure 2b, is significantly different than the predicted profile. The plasma data are from WIND [*Ogilvie et al.*, 1995] on DOY 77 and from ACE [*McComas et al.*, 1998] for the rest of the interval in Figure 2b. WIND/ACE observed a corotating stream, CRS-1, with a speed V ≈ 400 km/s on 22 March (81), as predicted for CH-1. ACE observed another corotating stream, CRS-2, with an average speed V ≈ 450 km/s on 27 March (86), which corresponds to the predicted stream from CH-2. However, instead of the predicted slow flow, WIND/ACE observed moderate speeds with three local peaks from 23 through 25 March (82–84). Moreover, ACE observed two streams that were not pre-

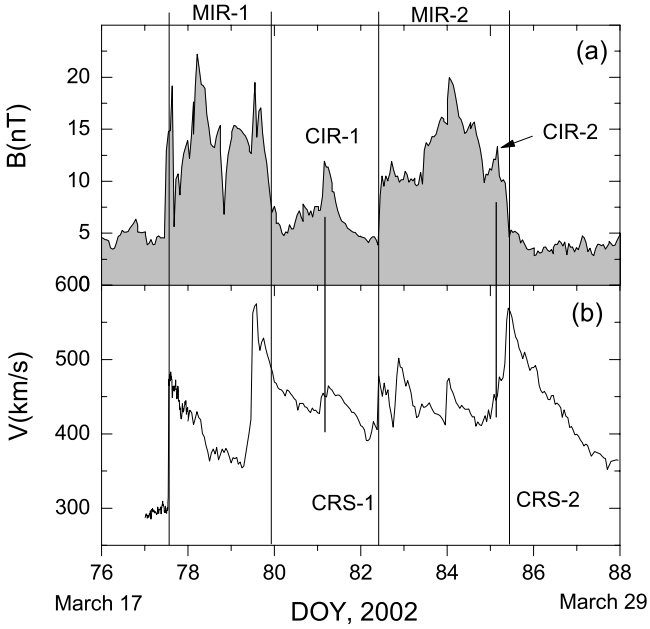

Figure 2. An overview of the magnetic field and plasma data at 1 AU from 17 to 29 March 2002. (a) The magnetic field strength profile showing two merged interaction regions, MIR-1 and MIR-2. (b) The speed profile showing two corotating streams, CRS-1 and CRS-2, and other flows that were not predicted by the potential field model. The two bold bars show the relations between the corotating interaction regions and the corotating streams.

dicted based on the solar data in Figure 1, on 18/19 March (77/78) and on 20/21 March (79/80).

[13] Typically, a corotating stream is associated with a corotating interaction region at the leading edge of the stream in which the maximum B $\approx$ 13–25 nT and the passage time is $\approx$4–16 hours [*Burlaga and King*, 1979]. Thus one might expect to see a simple magnetic field strength profile in the data at 1 AU, consisting of two narrow enhancements in B (with magnitudes $\approx$10 nT and widths $\approx$12 hours), one at the leading edge of each corotating stream, and a relatively constant field B $\approx$ 6 nT throughout the rest of the interval under consideration. The vertical bars in Figure 2 show the expected positions of these two narrow peaks.

[14] The observed magnetic field strength profile, B(t), (see the ACE data [*Smith et al.*, 1998] in Figure 2a) is very different than that expected from the discussion above. Instead of two isolated narrow peaks corresponding to the two "corotating interaction regions" (CIRs) there is only one isolated peak, CIR-1 associated with CRS-1. The narrow peak CIR-2 is part of a much broader region with strong magnetic fields, a merged interaction region MIR-2 (Figure 2a). The observed passage times of MIR-1 and MIR-2 are $\approx$2.5 and 3 days, respectively, much larger that those of the CIRs.

[15] We conclude that the two corotating streams predicted by the solar observations and the potential field maps in Figure 1 were observed at 1 AU. However, the observed speed profile contained other features that were not predicted. More importantly, the observed magnetic field strength profile is very different than that expected for the predicted streams. Instead of two narrow magnetic field strength enhancements correlated with speed and density profiles related to two corotating streams and CIRs, ACE observed two broad MIRs and one narrow isolated CIR between them. There was no correlation between B(t) in the MIRs and the speed profile, V(t).

3. Merged Interaction Regions

[16] Let us now determine why the magnetic field strength profile at 1 AU is so different from that predicted from the solar data. Our discussion is based on the plasma and magnetic field data from WIND for the interval 17 March (76) to 29 March (88). We consider $\approx$8.2 min averages of the magnetic field strength (B(nT)), elevation angle θ, and azimuthal angle ϕ measured by the magnetic field instrument on WIND [*Lepping et al.*, 1995]. The $\approx$8.2 min averages of speed V(km/s), density N(cm^{-3}), and proton temperature T(10^5°K) were measured by the SWE instrument on the WIND spacecraft [*Ogilvie et al.*, 1995]. The helium abundance, He^{4+}/H^{+} is from the SWEPAM instrument [*McComas et al.*, 1998] on ACE. The data are "level 2" data obtained from http://www.srl.caltech.edu/ACE/ASC/level2/lvl2DATA_SWEPAM.html. The instrument and data are discussed at http://www.srl.caltech.edu/ACE/ASC/level2/swepam_l2desc.html. Finally, we shall consider the ratio of O^{7+}/O^{6+} observed by the SWICS/SWIMS instrument [*Gloeckler et al.*, 1998] on ACE. The data are "level 2" data obtained from http://www.srl.caltech.edu/ACE/ASC/level2/lvl2DATA_SWEPAM.html. The instrument and data are discussed at http://www.srl.caltech.edu/ACE/ASC/level2/swics_swims_l2desc.html.

3.1. Merged Interaction Region-1

[17] MIR-1 moved past the WIND spacecraft from the middle of 18 March (77) to the beginning of 21 March (80) 2002 (Figure 3). Note that even on this scale there is no simple relation between B(t) and either N(t) or V(t). Thus one could not infer B(t) from measurements of N and V such as those obtained from remote sensing observations.

[18] The leading boundary of MIR-1 is a forward shock, "S1," indicated by a vertical line on 18 March (77) in Figure 3, across which there is an abrupt increase in B, V, N, and T. The shock S1 associated with CE-1 is relatively strong, the density increasing by a factor of >3 from $\approx$15 cm^{-3} to $\approx$50 cm^{-3}. Strongly fluctuating magnetic fields with a maximum strength $\approx$15 nT were observed for $\approx$12 hours following the passage of the shock on 18 March (77).

[19] The shock S1 was followed by a flow moving <400 km/s past the WIND spacecraft at 1 AU. The boundary between this flow and the sheath is not well defined; two possibilities are shown by vertical lines in Figure 3, one defined by the change in composition and the other by the change in magnetic field strength. This flow was still moving faster than the solar wind speed ahead of the shock, $\approx$375 km/s. The flow corresponds to complex ejecta (CE-1), as indicated by the relatively strong and variable magnetic fields that do not lie in the spiral field direction [*Burlaga et al.*, 2001, 2002] (Figures 3e and 3f) and the relatively high He^{4+}/H^{+} and O^{7+}/O^{6+} ratios in Figure 3g. For a

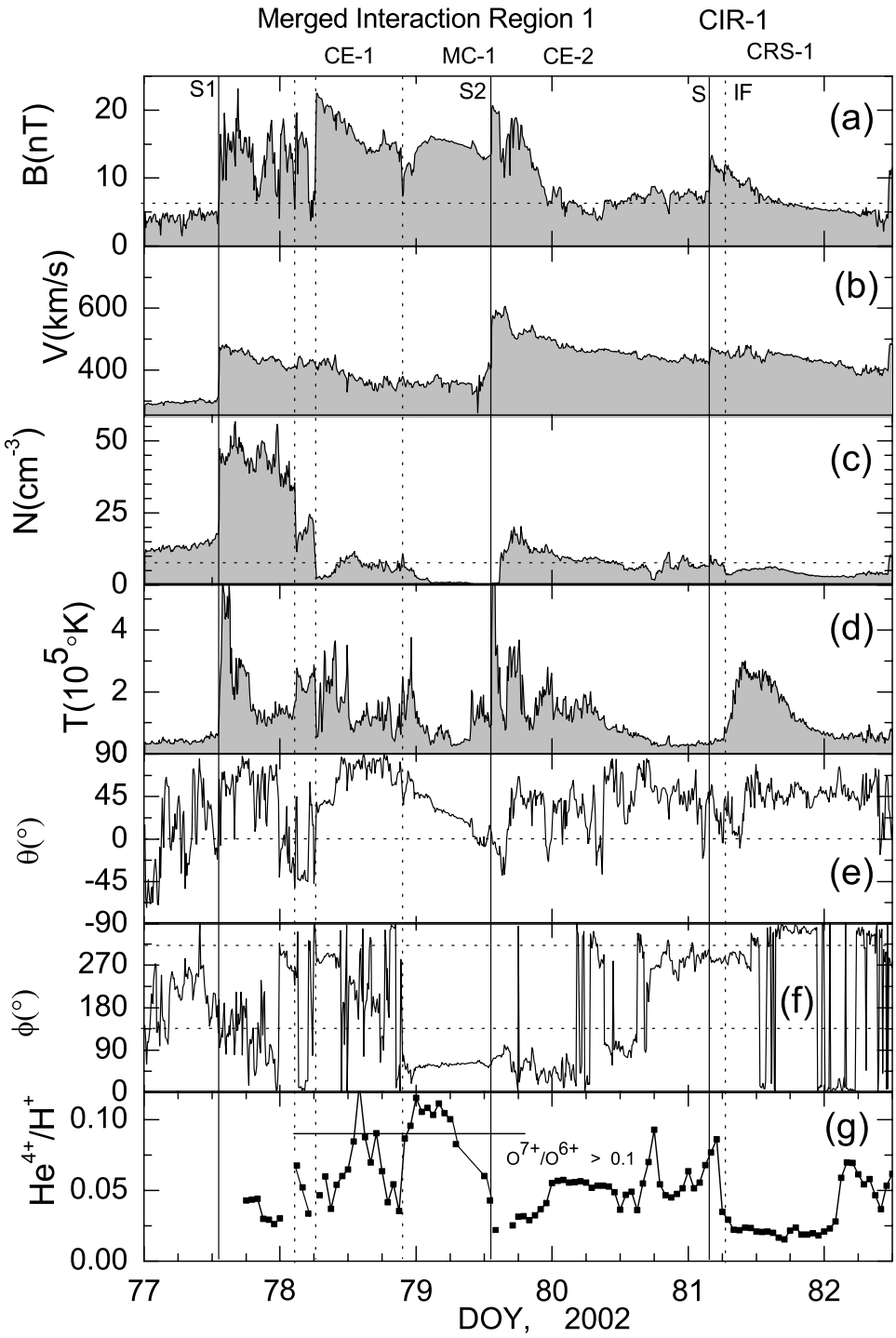

Figure 3. Plasma and magnetic field observations for MIR-1. (a-f) The magnetic field strength, solar wind speed, density, proton temperature, elevation angle of the magnetic field and azimuthal angle of the magnetic field, respectively. (g) The abundance ratios of He^{4+}/H^{+} (points) and an interval when $O^{7+}/O^{6+} > 0.1$ (horizontal line).

discussion of the composition signatures of ejecta, see *Hirshberg et al.* [1972], *Ogilvie* [1985], *Henke et al.* [1998], *Neugebauer* [1981], *Neugebauer and Goldstein* [1997], *Zurbuchen et al.* [2002], and *Zwickl et al.* [1983]. The density in CE-1 (Figure 3c) is near the average solar wind value, 6 cm^{-3}. Thus the momentum flux of CE-1, NV^2, is comparable to that of the average solar wind. However, the density in the sheath between the shock and CE-1 was very high, between 40 and 50 cm^{-3}, ≈7 or 8 times the average solar wind density. Of course, CE-1 could not be predicted from the quasi-steady solar magnetic field observations in Figure 1. It is likely that the complex ejecta that moved past 1 AU on 19 March (78) are related to the halo CME [*Howard et al.*, 1982; *Webb et al.*, 2000; *St. Cyr*

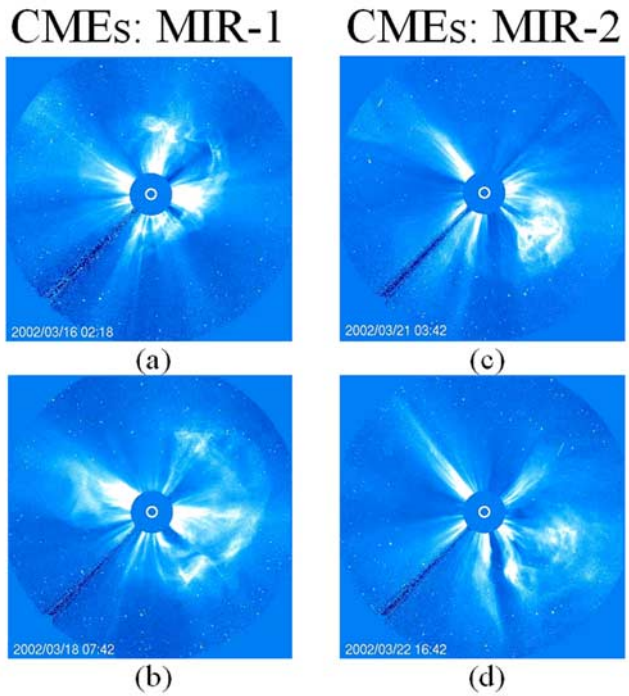

Figure 4. Coronal mass ejections (CMEs) associated with MIR-1 (a, b) and MIR-2 (c, d).

et al., 2000; *Plunkett et al.*, 1998] observed by the LASCO instrument on 15/16 March (74/75), 2002 (see Figure 4a and Table 1). Note that Figure 4 shows images from the LASCO C-3 field of view, whereas Table 1 is based on images from the C-2 field of view, closer to the Sun.

[20] The next component of MIR-1 in Figure 3 is a magnetic cloud that arrived at 1 AU near the beginning of 20 March (79). A magnetic cloud is a region containing strong B, low T, and a smooth rotation in the magnetic field direction as a magnetic cloud moves past 1 AU [*Burlaga et al.*, 1981]. The magnetic cloud was enriched in the ratio He^{4++}/H^{+} and $O^{7+}/O^{6+,}$ as indicated Figure 3g.

[21] The magnetic cloud was being overtaken by ejecta CE-2 (Figure 3) that began to move past WIND on approximately the beginning of 21 March (80). CE-2 probably did not contain strong magnetic fields, but it was driving a shock S2 that entered the rear of the magnetic cloud, as indicated by a vertical line on 20 March (79) in Figure 3. The magnetic field was strong for several hours in the sheath following the shock. CE-2 did not have a high O^{7+}/O^{6+} ratio, but there were two enhancements in He^{4++}/H^{+} at the rear of CE-2, which also had unusual and highly variable magnetic field directions. CE-2 was associated with a halo CME on 18 March (77) (see Figure 4b and Table 1). However, we cannot be certain that CE-2 is the interplanetary manifestation of that CME, owing to the limited observations. We cannot even be certain that CE-2 is related to only one CME. The same can be said of CE-1.

[22] The spatial configuration of the flows associated with MIR-1 is summarized in Figure 5a. The basic structures are those identified in Figure 3 and discussed above. The positions of the shocks and the front boundaries of the ejecta (to the extent that they can be identified subjectively) were estimated from the times that they were observed

Table 1. CMEs Associated With MIR-1 and MIR-2 During March 2002

DOY	Date	Time, UT	Location	PA, deg	V, km/s	Flare, peak	MIR	Ejecta
74	15 Mar	2306	S08 W03	307	911	23:10	1	CE-1
							1	MC-1
77	18 Mar	0254	S15 W22	311	989	2:31	1	CE-2
78	19 Mar	1154	S10 W58	259	698	12:31	2	CE-3
79	20 Mar	2354	S19 W60	242	1075	0:23	2	MC-2
81	22 Mar	1106	S20 W81	259	1750	11:14	2	CE-4

at 1 AU. Their positions in Figure 3 are estimated on the assumption that they were all propagating at a speed of ≈1 AU/4 days, ≈430 km/s. The shocks and the boundaries of ejecta are drawn as arcs of circles, since the actual shapes cannot be determined with observations from one spacecraft or two closely spaced spacecraft. In general, CMEs can accelerate and or decelerate in the corona [see, e.g., *Gopalswamy et al.*, 2000], but *Berdichevsky et al.* [2002] and *Lepping et al.* [2001, 2002] found that ejecta do not seem to change their overall speed between the Sun and 1 AU. More accurate transit speeds would require knowledge of how the objects decelerated and/or accelerated between the Sun and 1 AU, which cannot be determined from in situ observations at a single point. Thus, the structure illustrated in Figure 5a is only semiquantitative; the curves can be moved relative to one another, but the basic structure is roughly to scale. MIR-1 has a relatively large radial extent ≈2/3 AU.

[23] We infer that the magnetic fields in MIR-1 consisted of the following components: (1) compressed, highly variable magnetic fields in the sheath between CE-1 and its shock S1; (2) strong magnetic fields carried by CE-1; (3) strong magnetic fields within a magnetic cloud; and (4) compressed magnetic fields behind a shock S2 driven by CE-2 that was advancing into the magnetic cloud. The magnetic field was not strong in CE-2. The compression of the strong magnetic fields in a magnetic cloud by a shock

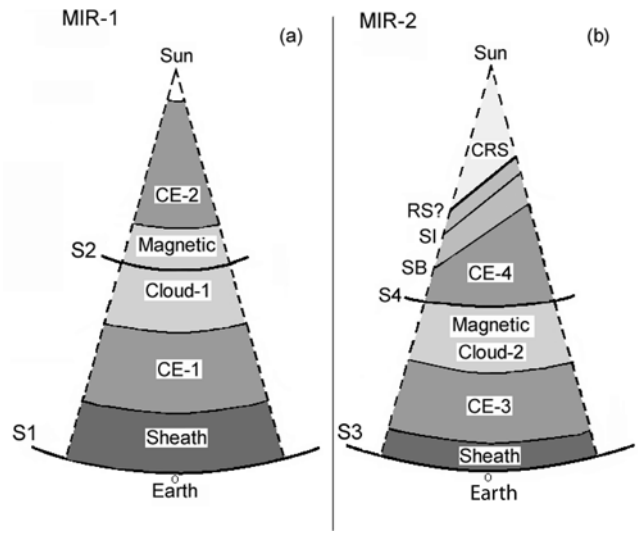

Figure 5. The configurations of the flows and shocks associated with MIR-1 (a) and MIR-2 (b).

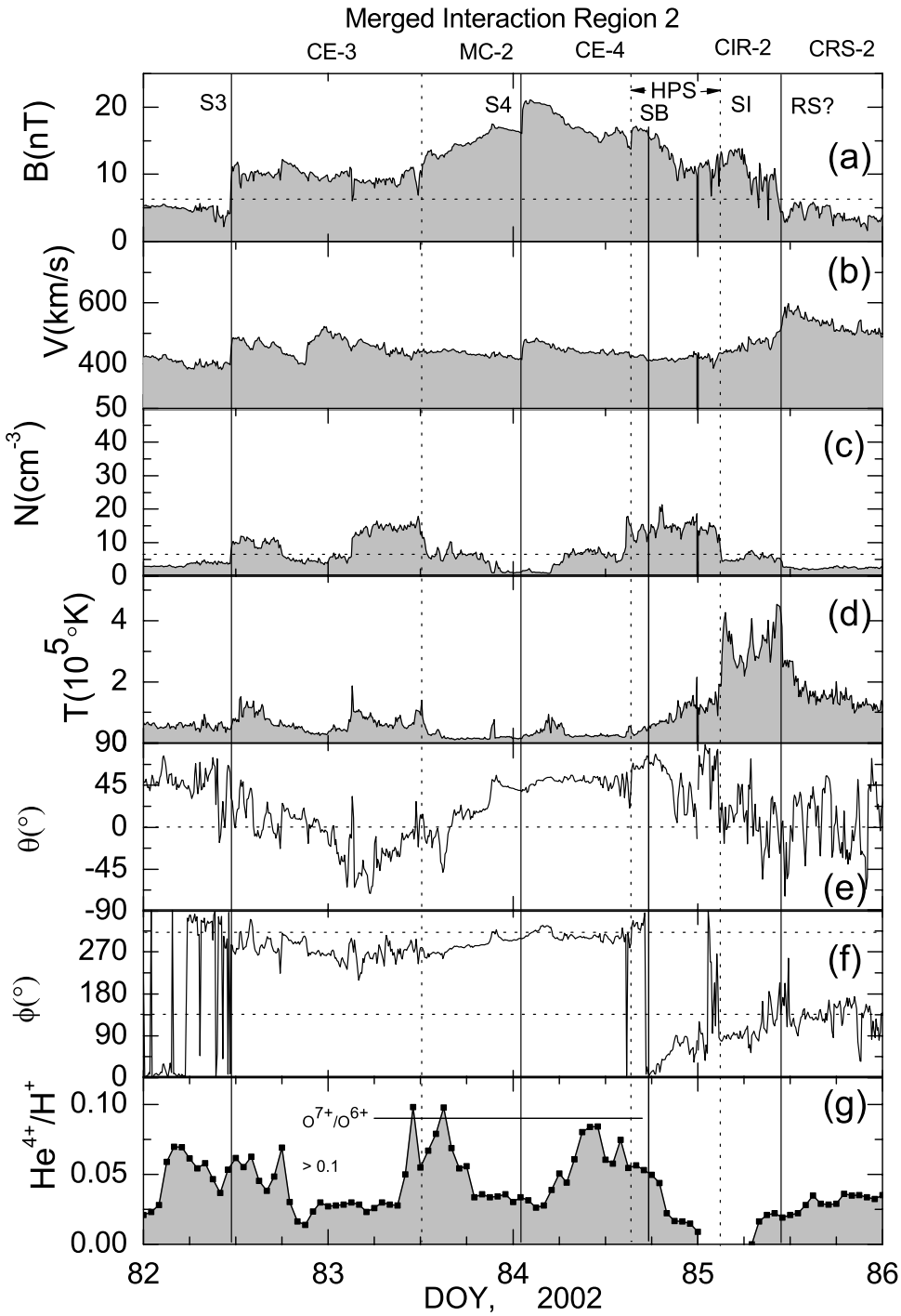

Figure 6. Plasma and magnetic field observations for MIR-2. (a-g) The same meaning as in Figure 3.

passing through the magnetic cloud can have significant geomagnetic effects [*Burlaga et al.*, 1987].

3.2. Merged Interaction Region-2

[24] MIR-2 moved past the WIND and ACE spacecraft from the middle of 23 March through the first half of 26 March 2002 (82–85) (Figure 6). Again, there is no relation between B(t) and either V(t) or N(t) in the MIR.

[25] The MIR-2 was bounded on front by a shock S3 shown by a vertical line on DOY 82 in Figure 6. The shock was probably driven by ejecta, CE-3, whose arrival might coincide with the increase in V on DOY 82 shown in Figure 6b. There were enhancements in He^{4++}/H^{+} and O^{7+}/O^{6+} on DOY 83, consistent with the passage of ejecta. MIR-2 was associated with at least three earthward moving CMEs observed by LASCO from the middle of 19 March (78) through the middle of 22 March (81) (see Table 1). However, it is difficult to make a one-to-one correspondence between the ejecta in MIR-2 and CMEs observed by LASCO. CE-3 was possibly associated with a CME on 19/20 March (78/79).

[26] A magnetic cloud (MC-2) was overtaking CE-3, and its antisunward boundary moved past 1 AU on 24 March

(83.5), as indicated by a vertical dashed line in Figure 6. The magnetic cloud was moving at a moderate speed, ≈400 km/s, and it was an "old" magnetic cloud in the sense that it was not expanding at 1 AU (the signature of which is a decreasing speed profile as the magnetic cloud moved past 1 AU). There was an enhancement in He^{4++}/H^{+} and O^{7+}/O^{6+} within the magnetic cloud (Figure 6g). The magnetic cloud might be related to the CME observed on 20/21 March (79/80) (see Figure 4b and Table 1).

[27] A shock, S4, was moving through the rear of the magnetic cloud and passed 1 AU at the beginning of 25 March (84) (Figure 6). This shock was related to slowly moving ejecta, CE-4 on DOY 84, in which there was an enhancement in He^{4++}/H^{+} and O^{7+}/O^{6+}. CE-4 is related to a CME observed on 22 March (81) (Figure 4d and Table 1). Radio wave observations from WIND suggest that the CME was driving a shock in the corona, which could be the shock S4. A second CME was also observed on 22 March (81) (Table 1). We cannot determine whether it overtook and merged with the first CME to form CE-4 or whether it was not intercepted by WIND.

[28] A sector boundary (SB) moved past WIND on 25 March (84.75) (Figure 6f). This corresponds to the neutral line on the Sun that crossed the subsolar point on 21 March (80) (see the middle panel of Figure 1). The SB was embedded in a high density, slow speed flow (Figures 6c and 6b) across which the magnetic field direction rotated from one sector to the next over a period of ≈9 hours as the material moved past 1 AU. This region might be the heliospheric plasma sheet (HPS). This interpretation is supported by the observations of a relatively low He^{4++}/H^{+} ratio, which is characteristically observed near sector boundaries [*Borrini et al.*, 1981; *Gosling et al.*, 1981]. *Burlaga et al.* [1990] identified the HPS as a region with high N, low V and entropy that is relatively thick (passage time of the order of several hours or more), as observed here. On the other hand, *Winterhalter et al.* [1994] suggested that the HPS is very thin (passage time of the order of a minute). It is possible that Winterhalter et al., were mistakenly identifying the HPS with a magnetic hole, since magnetic holes are often seen at or near a SB and the density is typically high in a magnetic hole [*Klein and Burlaga*, 1980]. The HPS was bounded on the sunward side by a stream interface (SI), defined by an abrupt decrease in density and abrupt increase in proton temperature in front of a corotating stream [*Burlaga*, 1974] that moved past 1 AU on DOY 84.15 (Figure 6). The corotating stream, with the characteristically low N and high T, was observed on the second half of DOY 85. This corotating stream, CRS-2, corresponds to the coronal hole CH-2 in Figure 1.

[29] The spatial configuration of the flows associated with MIR-2 is summarized in Figure 5b. The basic structures are those identified in Figure 6. As in the case of MIR-1 discussed above, the positions of the shocks and the front boundaries of the ejecta were estimated from the times that they were observed at 1 AU (see Figure 6) with the assumption that they were all propagating at a speed of ≈1 AU/4 days, 430 km/s. Figure 5b shows that MIR-2 was related to at least three ejecta (including a magnetic cloud), the HPS and a corotating stream. A shock S3 was driven by ejecta CE-3, and a sheath was observed between S3 and CE-3. A magnetic cloud was overtaking and interacting with CE-3, and it was being overtaken by ejecta CE-4 that was driving a shock S4 which was probably propagating into the rear of the magnetic cloud. The front boundary of CE-4 could not be identified with certainty. The rear boundary of CE-4 was probably at the HPS, which contained the sector boundary SB. A corotating stream CRS-2, which might have compressed the material in the HPS, was overtaking the sector boundary. The CRS-2 was bounded in front by a stream interface (SI-2), and it produced a corotating interaction region that was bounded in the rear by an abrupt change that had the signature of a reverse corotating shock, marking the sunward boundary of MIR-2. MIR-2 had a radial extent ≈3/4 AU, somewhat larger than that of MIR-1.

4. Geomagnetic Effects of the Merged Interaction Regions

[30] It is well known that geomagnetic activity, measured by the Dst index, is related to the passage of fast flows in which the interplanetary magnetic field has a significant southward component and to narrow regions in which the momentum flux is relatively high. Southward magnetic fields in fast flows cause a decrease in Dst, and a pulse in the momentum flux causes an increase in Dst [*Akasofu and Chapman*, 1972]. It is usually assumed that a geomagnetic storm is associated with a single transient flow [*Lyatsky and Tan*, 2003]. However, interactions among flows and shocks can amplify these geoeffective quantities [*Burlaga et al.*, 1987]. Thus one might expect that MIRs can be associated with relatively long intervals of increased geomagnetic activity, at least when they contain southward directed magnetic fields.

[31] Figure 7 shows how Dst varied during the interval containing the two MIRs that we have discussed above. The Dst index is plotted in Figure 7a, and the MIRs can be seen in the profile of the magnetic field strength that is plotted in Figure 7b. The momentum flux and the B_z component of the magnetic field are plotted in Figures 7c and 7d, respectively; the magnetic field is in heliographic coordinates [*Burlaga*, 1995, Figure 1.1]. Figures 7a and 7b show that each of the MIRs was associated with a geomagnetic storm lasting ≈3 days.

[32] Storm-1, associated with MIR-1, began with a large, abrupt increase in Dst associated with the very large increase in momentum flux across the shock S1, which was caused by the high densities behind the shock. Dst decreased when the magnetic field turned southward, and Dst remained below 0 throughout most of the passage of MIR-1 even when the magnetic field was northward. Finally, Dst increased abruptly following the shock S2, which was near the end of MIR-1. Storm-1 lasted ≈2.5 days, which is longer than a typical magnetic storm [*Lockwood*, 1971].

[33] Storm-2, associated with MIR-2, began with a relatively small increase in Dst associated with a small increase in momentum flux across the shock S3. Dst decreased to moderately low levels (Dst < 100) when the magnetic field turned southward, and it remained low throughout the rest of the passage of MIR-2, even when the magnetic field was northward. During the recovery of storm-2, there was a spike in Dst related to the shock S4. Storm-2 lasted ≈3 days, again longer than a typical magnetic storm.

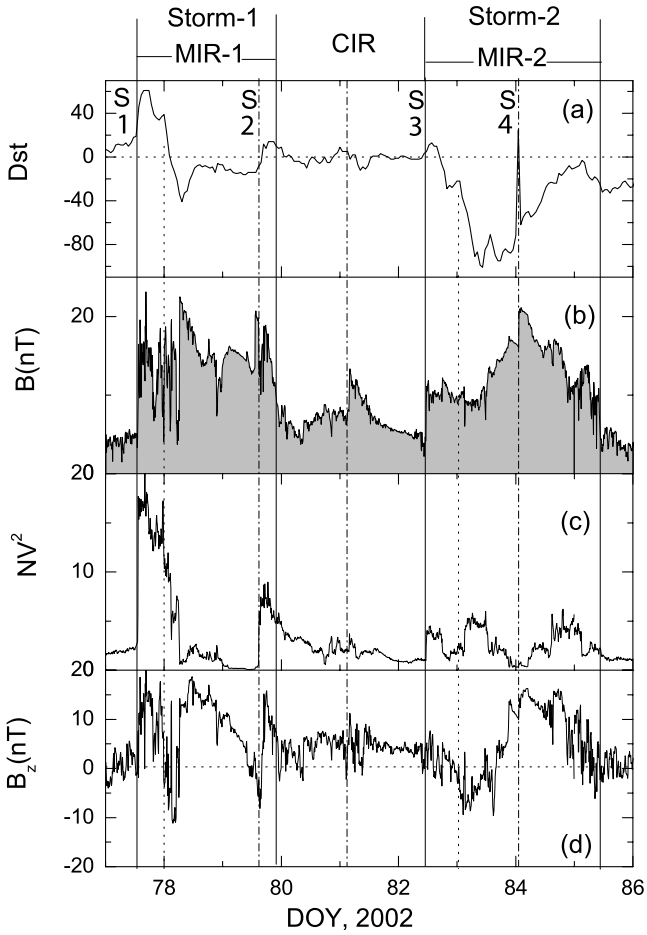

Figure 7. The merged interaction regions MIR-1 and MIR-2, identified by the magnetic field strength profile (b) caused two magnetic storms identified by the Dst index (a). Peaks in the momentum flux NV^2 (c) caused increases in Dst, and decreases in B_z caused decreases in Dst (d).

[34] During the 2.5 days between MIR-1 and MIR-2, Dst was approximately zero, despite the passage of the corotating stream and CIR on DOY 81. The magnetic field was northward throughout this geomagnetically quiet interval.

[35] The two MIRs discussed above were chosen on the basis of solar wind observations alone, without consideration of geomagnetic effects. It happens that B_z was northward throughout most of the two MIRs we selected, and the associated geomagnetic activity was therefore moderate. In general, there will exist MIRs in the solar wind in which B_z is primarily southward, and interactions among flows can cause significant amplification in B_z in these MIRs [*Burlaga et al.*, 1987]. Such MIRs can cause major prolonged geomagnetic storms. A typical magnetic storm, caused by a magnetic cloud for example, lasts of the order of 1/2 day [*Zhang and Burlaga*, 1988].

5. Effects of the Merged Interaction Regions on Cosmic Rays

[36] Typically, a Forbush decrease at 1 AU is an asymmetric worldwide depression in cosmic ray intensity recorded by neutron monitors at 1 AU lasting several days [*Parker*, 1963; *Lockwood*, 1971]. The major portion of the decrease phase is completed within 12–24 hours, and the recovery phase of a Forbush decrease generally lasts several days [*Lockwood*, 1971]. *Barouch and Burlaga* [1975] showed that Forbush decreases at 1 AU are related to enhancements in the interplanetary magnetic field strength and shocks. An association between systems of transient flows, MIRs, and long-lasting decreases in the cosmic ray intensity was observed by *Burlaga et al.* [1984, 1985b].

[37] Figure 8a shows the cosmic ray rate measured by the Oulu neutron monitor (available at http://cosmicrays.oulu.fi/#database) for the period DOY 77–88 discussed above and extending through DOY 95, 2002. The neutron monitor counting rate shows a Forbush decrease from DOY 77.5–94.5. The decrease phase lasted 8 days, which is an order of magnitude greater than a typical decrease phase. The recovery phase lasted 9 days, which is slightly larger than the typical recovery phase.

[38] The structure of this Forbush decrease is related to a series of flows and shocks, rather than a single transient flow. The unusually long decrease phase was caused by the two closely separated MIRs (Figure 8). A large decrease in the cosmic ray intensity was associated with the passage of MIR-1, and a further decrease occurred during the passage of MIR-2. The cosmic ray intensity showed no net decrease

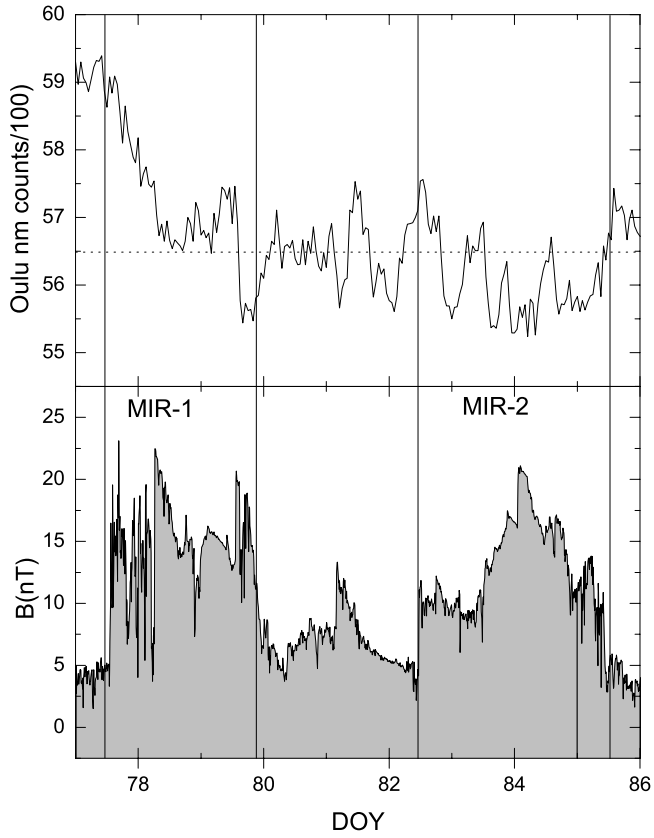

Figure 8. A Forbush decrease with the relatively long decrease phase (a) was caused by the two MIRs, as shown in the magnetic field strength profile (b). The recovery (not shown) was associated with two corotating streams.

during the passage of the flows between the two MIRs. The recovery of the cosmic ray counting rate occurred during the passage of two corotating streams, namely, CRS-2 and a large, fast corotating stream associated with a large equatorial coronal hole that falls outside the range of Figure 1. The recovery was related to entry of Earth into the region occupied by two corotating streams, which had an angular extent of $\approx 120^\circ$. Cosmic rays from large distances have relatively free access to 1 AU along the spiral magnetic field lines in corotating streams. The cosmic rays did not have to diffuse through MIRs, although the MIRs, particularly the shocks, probably influenced the recovery phase as well as the decrease phase. To our knowledge, there are no models of Forbush decreases related to complicated flow configurations and MIRs such as those discussed in this paper.

6. Summary and Discussion

[39] We identified two merged interaction regions (MIR-1 and MIR-2) at 1 AU during the interval from 18 March through 28 March (77 through 87) 2002, and we discussed their probable structure and origin in terms of interacting flows and shocks. The observations were made near a single point at 1 AU as the MIRs moved past a spacecraft. MIR-1 and MIR-2 were relatively large structures, moving past Earth in ≈ 2.5 and 3 days, respectively, corresponding to radial dimensions $\approx 2/3$ and 3/4 AU, respectively.

[40] MIR-1 formed by interactions involving at least two complex ejecta (CE), a magnetic cloud, and two shocks. One CE was associated with a shock that interacted with a magnetic cloud ahead of it (farther from the Sun). The shock entered the magnetic cloud, compressing the magnetic fields in the rear of the magnetic cloud. The magnetic cloud was overtaking and interacting with a second CE that was also associated with a shock. The magnetic field in the sheath between the shock and the CE was strong, and the density behind the shock was very high.

[41] If we had observations of the speed (V) and density (N) such as those that will be obtained by the coronagraph and the heliospheric imager that will be flown on STEREO, we could have presented a more definitive and quantitative discussion of the structure of MIR-1. Moreover, we could have followed its formation and evolution as its components moved and interacted between the Sun and Earth. The origin and evolution of the strong shock at the beginning of MIR-1 and the very high densities in the sheath behind the shock could have been determined unambiguously. The nature of CE-1, which seems unusual, might be better understood if we could have followed its motion from the Sun. The interaction between CE-1 and its shock on the one hand and the magnetic cloud on the other could have been studied as a function of time as they moved from the Sun to Earth. The CMEs associated with the two ejecta in MIR-1 could have been identified and their paths could have been measured using STEREO observations, rather than being inferred from the images of halo CMEs made from a single point. The CME related to the magnetic cloud might have been determined, and the interaction of the magnetic cloud with the ejecta ahead of it could have been followed as the magnetic cloud moved to 1 AU.

[42] MIR-2 was related to a corotating stream, the heliospheric plasma sheet (HPS), two complex ejecta, a magnetic cloud, and at least two shocks. The corotating stream was overtaking the HPS and CE, compressing the magnetic field in the HPS. There were strong magnetic fields at the leading edge of the corotating stream and possibly a corotating reverse shock forming the sunward boundary of MIR-2. The CE was driving a shock that entered the rear of a magnetic cloud, compressing its relatively strong fields. The magnetic cloud was overtaking another CE that was driving a shock. The magnetic field was strong in the sheath behind the shock and CE as well as in the CE itself.

[43] It is important to understand that MIRs are dynamic structures. A MIR can evolve significantly even during the several days during which it moves to and past 1 AU. More importantly, the structure of a MIR is determined by the nonlinear evolution of distinct flows and shocks between the Sun and Earth. Memory of the conditions near the Sun is lost in the process. Thus one cannot unambiguously determine the structure of a MIR and the manner in which it formed using observations from a single spacecraft at 1 AU. It is necessary to follow the dynamical evolution of these flows and the formation of MIRs continuously from the Sun to 1 AU. It is even possible that a CE observed at 1 AU is formed by the merging of two or more CMEs and that a single shock at 1 AU is formed by the merging of two shocks between the Sun and 1 AU.

[44] Assume that we had observations of the speed (V) and density (N) such as those that will be obtained by STEREO. From the coronagraph images and the heliospheric imager we could have determined whether all or some of the CMEs seen by LASCO did in fact move past WIND and ACE. From the heliospheric imager we could have identified the shocks near the Sun and determined whether some shocks merged en route to Earth. The heliosphere imager could also have identified the heliospheric plasma sheet and the corotating interaction region and followed their motions as they overtook and merged with MIR-2. Information from the instruments such as those on STEREO and SMEI together with other solar observations and other in situ observations might also have revealed additional complexity in the structures and interactions involved in the formation of MIR-2 that we did not identify in our analysis of more limited observations.

[45] One of the most significant limitations of current and planned instruments for the study of the solar wind is the inability to make remote observations of the magnetic field in the solar wind and the corona. STEREO, SMEI, and interplanetary scintillation observations cannot measure the evolution of magnetic fields leading to the formation of merged interactions, and they cannot provide direct knowledge of magnetic field profiles such as those discussed in this paper. There is no general relation between the profiles B(t), V(t), and N(t) in MIRs such as that in corotating streams. Thus one cannot use remote sensing observations of density and speed to infer B(t). It is important to develop MHD models that can describe complicated interactions such as those discussed in this paper that lead to the formation of MIRs.

[46] The interactions that produce MIRs can produce configurations that cause greater geomagnetic effects than a single shock, magnetic cloud, or any other isolated structure. Thus MIRs provide a new perspective for the study of geomagnetic activity. MIRs and successive MIRs

can also produce Forbush decreases with relatively long decrease phases at 1 AU, followed by a recovery related to corotating streams that "rotate" past Earth after the MIRs move into the outer heliosphere. Thus models of such Forbush decreases must consider MIRs and several interacting flows (possibly including both ejecta and corotating streams), as opposed to the conventional model of a Forbush decrease as the result of the passage of complex ejecta or a magnetic cloud. Perhaps some day it will be possible to calculate the evolving spatial distribution of cosmic rays and low energy particles associated with MIRs and interacting flows.

[47] **Acknowledgments.** Most of the in situ data used in this paper were placed on the internet by the Principal Investigators of the respective experiments. Solar wind and alpha particle data from ACE are from the experiment of D. McComas, and the oxygen data are from the instrument of G. Gloeckler on ACE. The WIND and ACE magnetic field data are from R. Lepping and C. Smith, respectively. K. Ogilvie provided the WIND plasma data.

[48] Shadia Rifai Habbal thanks Arjun Tan and David Webb for their assistance in evaluating this paper.

References

Akasofu, S.-I., and S. Chapman, *Solar-Terrestrial Physics*, p. 506, Clarendon Press, New York, 1972.

Altschuler, M. D., and G. J. Newkirk, Magnetic fields and the structure of the solar corona, *Solar Phys.*, *9*, 131, 1969.

Barouch, E., and L. F. Burlaga, Causes of Forbush decreases and other cosmic ray variations, *J. Geophys. Res.*, *80*, 449–456, 1975.

Behannon, K. W., L. F. Burlaga, and A. Hewish, Structure and evolution of compound streams at less than or equal to 1 AU, *J. Geophys. Res.*, *96*, 21,213–21,225, 1991.

Berdichevsky, D., et al., Evidence for multiple ejecta; April 7–11, 1997 ISTP Sun-Earth connection event, *Geophys. Res. Lett.*, *25*, 2473–2476, 1998.

Berdichevsky, D. B., C. J. Farrugia, B. J. Thompson, R. P. Lepping, D. Reames, M. L. Kaiser, J. T. Steinberg, S. P. Plunkett, and D. Michels, Halo-coronal mass ejections near the 23rd solar minimum: Lift-off at the Sun, interplanetary tracking, and in-situ observations at 1 AU, *Ann. Geophys.*, *20*, 891–916, 2002.

Berdichevsky, D. B., C. J. Farrugia, R. P. Lepping, I. G. Richardson, A. B. Galvin, R. Schwenn, D. V. Reames, K. W. Ogilvie, and M. L. Kaiser, Solar-heliospheric-magnetospheric observations on March 23–April 26, 2001: Similarities to observations in April 1979, *Solar Wind Ten*, edited by M. Velli et al., *AIP Conf. Proc.*, *679*, 758–761, 2003.

Borrini, G., J. T. Gosling, S. J. Bame, W. C. Feldman, and J. M. Wilcox, Solar wind helium and hydrogen structure near the heliospheric current sheet—A signal of coronal streamers at 1 AU, *J. Geophys. Res.*, *86*, 4565–4573, 1981.

Brueckner, G. E., et al., The large angle spectroscopic coronagraph LASCO, *Sol. Phys.*, *162*, 357–402, 1995.

Burlaga, L. F., Interplanetary stream interfaces, *J. Geophys. Res.*, *79*, 3717, 1974.

Burlaga, L. F., *Interplanetary Magnetohydrodynamics*, Oxford Univ. Press, New York, 1995.

Burlaga, L. F., and J. H. King, Intense interplanetary magnetic fields observed by geocentric spacecraft during 1963–1975, *J. Geophys. Res.*, *84*, 6684, 1979.

Burlaga, L. F., and K. W. Ogilvie, Magnetic and thermal pressures in the solar wind, *Sol. Phys.*, *15*, 61, 1970.

Burlaga, L. F., E. Sittler, F. Mariani, and R. Schwenn, Magnetic loop behind an interplanetary shock: Voyager, Helios, and IMP-8 observations, *J. Geophys. Res.*, *86*, 6673, 1981.

Burlaga, L. F., R. Schwenn, and H. Rosenbauer, Dynamical evolution of interplanetary magnetic-fields and flows between 0.3-AU and 8.5-AU: Entrainment, *Geophys. Res. Lett.*, *10*, 413–416, 1983.

Burlaga, L. F., F. B. McDonald, N. F. Ness, R. Schwenn, A. J. Lazarus, and F. Mariani, Interplanetary flow systems associated with cosmic ray modulation in 1977–1980, *J. Geophys. Res.*, *89*, 6579–6587, 1984.

Burlaga, L. F., F. B. McDonald, M. L. Goldstein, and A. J. Lazarus, Cosmic ray modulation and turbulent interaction regions near 11 AU, *J. Geophys. Res.*, *90*, 2027–2039, 1985a.

Burlaga, L. F., V. Pizzo, A. Lazarus, and P. Gazis, Stream dynamics between 1 AU and 2 AU: A comparison of observations and theory, *J. Geophys. Res.*, *90*, 7377, 1985b.

Burlaga, L. F., K. W. Behannon, and L. W. Klein, Compound streams, magnetic clouds, and major geomagnetic storms, *J. Geophys. Res.*, *92*, 5725–5734, 1987.

Burlaga, L. F., W. H. Mish, and Y. C. Whang, Coalescence of recurrent streams of different sizes and amplitudes, *J. Geophys. Res.*, *95*, 4247–4255, 1990.

Burlaga, L. F., R. Skoug, C. W. Smith, and D. F. Webb, Fast ejecta during the ascending phase of solar cycle 23: ACE observations, 1998–1999, *J. Geophys. Res.*, *106*, 20,957–20,977, 2001.

Burlaga, L. F., S. Plunkett, and C. St. Cyr, Successive CMEs and complex ejecta, *J. Geophys. Res.*, *107*, 1266, 2002.

Cane, H. V., and I. G. Richardson, Interplanetary coronal mass ejections in the near-Earth solar wind during 1996–2002, *J. Geophys. Res.*, *108*(A4), 1156, doi:10.1029/2002JA009817, 2003.

Cane, H. V., I. G. Richardson, and O. C. St. Cyr, Coronal mass ejections, interplanetary ejecta, and geomagnetic storms, *Geophys. Res. Lett.*, *27*, 3591–3594, 2000.

Gloeckler, G., et al., Investigation of the composition of solar and interstellar matter using solar wind and pickup ion measurements with SWICS and SWIS on the ACE spacecraft, *Space Sci. Rev.*, *86*(1–4), 492–539, 1998.

Gopalswamy, N., A. Lara, R. P. Lepping, M. L. Kaiser, D. Berdichevsky, and O. C. St. Cyr, Effective interplanetary acceleration of coronal mass ejections, *Geophys. Res. Lett.*, *27*, 145–148, 2000.

Gopalswamy, N., S. Yashiro, M. L. Kaiser, R. A. Howard, and J. L. Bougeret, Radio signatures of coronal mass ejection interaction: Coronal mass ejection cannibalism?, *Astrophys. J.*, *548*(1), L91–L94, 2001.

Gosling, J. T., Corotating and transient solar wind flows in three dimensions, *Annu. Rev. Astron. Astrophys.*, *34*, 35–73, 1996.

Gosling, J. T., Coronal mass ejections: An overview, in *Coronal Mass Ejections*, *Geophys. Monogr. Ser.*, vol. 99, edited by N. Crooker, J. A. Joselyn, and J. Feynman, pp. 9, AGU, Washington, D.C., 1997.

Gosling, J. T., G. Borrini, J. R. Asbridge, S. J. Bame, W. C. Feldman, and R. T. Hansen, Coronal streamers in the solar wind at 1-AU, *J. Geophys. Res.*, *86*, 5438–5448, 1981.

Henke, T., J. Woch, U. Mall, S. Livi, B. Wilken, R. Schwenn, G. Gloeckler, R. von Steiger, R. J. Forsyth, and A. Balogh, Differences in the O^{7+}/O^{6+} ratio of magnetic cloud and noncloud coronal mass ejections, *Geophys. Res. Lett.*, *25*, 3465–3468, 1998.

Hirshberg, J., S. J. Bame, and E. E. Robbins, Solar flares and helium enrichments, *Solar Phys.*, *23*, 467, 1972.

Howard, R. A., D. J. Michels, N. R. Sheeley, and M. J. Koomen, The observation of a coronal transient directed at Earth, *Ap. J.*, *263*, L101–104, 1982.

Hundhausen, A. J., *Coronal Expansion and Solar Wind*, Springer-Verlag, New York, 1972.

Hundhausen, A. J., An interplanetary view of coronal holes, in *Coronal Holes and High Speed Wind Streams*, edited by J. B. Zirker, pp. 225–329, Colo. Assoc. Univ. Press, Boulder, Colo., 1977.

Hundhausen, A. J., Coronal mass ejections, in *The Many Faces of the Sun*, edited by K. T. Strong et al., pp 143–200, Springer-Verlag, New York, 1999.

Jackson, B. V., and P. P. Hick, Corotational tomography of heliospheric features using global Thomson scattering data, *Sol. Phys.*, *211*(1–2), 345–356, 2002.

Klein, L., and L. F. Burlaga, Interplanetary sector boundaries 1971–1973, *J. Geophys. Res.*, *85*, 2269–2276, 1980.

Lepping, R., et al., The Wind magnetic field investigation, *Space Sci. Rev.*, *71*, 207–229, 1995.

Lepping, R. P., et al., The Bastille day magnetic clouds and upstream shocks: Near Earth interplanetary observations, *Sol. Phys.*, *204*, 287–305, 2001.

Lepping, R. P., D. Berdichevsky, A. Szabo, A. J. Lazarus, and B. J. Thompson, Upstream shocks and interplanetary magnetic cloud speed and expansion: Sun, wind, and Earth observations, in *Space Weather Study Using Multipoint Techniques, Proc. of COSPAR Symp.*, vol. 26, edited by L.-H. Lyu, pp. 87–96, Pergamon, New York, 2002.

Lockwood, J. A., Forbush decreases in cosmic radiation, *Space Sci. Rev.*, *12*, 658–715, 1971.

Lyatsky, W., and A. Tan, Solar wind disturbances responsible for geomagnetic storms, *J. Geophys. Res.*, *108*(A3), 1134, doi:10.1029/2001JA005057, 2003.

McComas, D. J., S. J. Bame, P. Barker, W. C. Feldman, J. L. Phillips, P. Riley, and J. W. Griffee, Solar wind electron proton alpha monitor (SWEPAM) for the Advanced Composition Explorer, *Space Sci. Rev.*, *86*(1–4), 563–612, 1998.

Neugebauer, M., Observations of solar wind helium, *Fund. Cosmic Phys.*, *7*, 131, 1981.

Neugebauer, M., and R. Goldstein, Particle and field signatures of coronal mass ejections in the solar wind, in *Coronal Mass Ejections*, *Geophys. Monogr. Ser.*, vol. 99, edited by N. Crooker, J. A. Joselyn, and J. Feynman, pp. 245, AGU, Washington, D.C., 1997.

Neugebauer, M., and P. C. Liewer, Creation and destruction of transitory coronal holes and their fast solar wind streams, *J. Geophys. Res.*, *108*(A1), 1013, doi:10.1029/2002JA009326, 2003.

Neugebauer, M., P. C. Liewer, E. J. Smith, R. Skoug, and T. H. Zurbuchen, Sources of the solar wind at solar activity maximum, *J. Geophys. Res.*, *107*(A12), 1488, doi:10.1029/2001JA000306, 2002.

Ogilvie, K. W., Analysis of O^{7+}/O^{6+} Observations in the Solar Wind, *J. Geophys. Res.*, *90*, 9881–9884, 1985.

Ogilvie, K., et al., SWE, A comprehensive plasma instrument for the Wind spacecraft, *Space Sci. Rev.*, *71*, 55–77, 1995.

Parker, E. N., *Interplanetary Dynamical Processes*, Wiley-Interscience, New York, 1963.

Plunkett, S. P., B. J. Thompson, R. A. Howard, D. J. Michels, O. C. St. Cyr, S. J. Tappin, R. Schwenn, and P. L. Lamy, Observations of an Earth-directed coronal mass ejection on May 12, 1997, *Geophys. Res. Lett.*, *25*, 2477–2480, 1998.

Schatten, K. H., J. M. Wilcox, and N. F. Ness, A model of the interplanetary and coronal magnetic fields, *Solar Phys.*, *6*, 442–445, 1969.

Schwenn, R., Large-scale structure of the interplanetary medium, in *Physics of the Inner Heliosphere*, edited by R. Schwenn and E. Marsch pp. 99–171, Springer-Verlag, New York, 1991.

Sheeley, N. R., and Y. M. Wang, Magnetic field configurations associated with fast solar wind, *Sol. Phys.*, *131*(1), 165–186, 1991.

Smith, C. W., J. L. L'Heureux, N. F. Ness, M. H. Acuña, L. F. Burlaga, and J. Scheifele, The ACE magnetic field experiment, *Space Sci. Rev.*, *86*, 613–632, 1998.

St. Cyr, O. C., et al., Properties of coronal mass ejections: SOHO LASCO observations from January 1996 to June 1998, *J. Geophys. Res.*, *105*, 18,169–18,185, 2000.

Wang, Y.-M., and N. R. Sheeley Jr., The high-latitude solar wind near sunspot maximum, *Geophys. Res. Lett.*, *24*, 3141, 1997.

Wang, Y. M., N. R. Sheeley, J. L. Phillips, and B. E. Goldstein, Solar wind stream interactions and the wind speed-expansion factor relationship, *Ap. J.*, *488*(1), L51, 1997.

Webb, D. F., E. W. Cliver, N. U. Crooker, O. C. St. Cyr, and B. J. Thompson, The relationship of halo CMEs, magnetic clouds, and magnetic storms, *J. Geophys. Res.*, *105*, 7491–7508, 2000.

Winterhalter, D., E. J. Smith, M. E. Burton, N. Murphy, and D. J. McComas, The heliospheric plasma sheet, *J. Geophys. Res.*, *99*, 6667–6680, 1994.

Zhang, G., and L. F. Burlaga, Magnetic clouds, geomagnetic disturbances, and cosmic ray decreases, *J. Geophys. Res.*, *93*, 2511–2518, 1988.

Zurbuchen, T. H., L. A. Fisk, G. Gloeckler, and R. von Steiger, The solar wind composition throughout the solar cycle, *Geophys. Res. Lett.*, *29*, 1352, 2002.

Zwickl, R. D., J. R. Asbridge, S. J. Bame, W. C. Feldman, J. T. Gosling, and E. J. Smith, Plasma properties of driver gas following interplanetary shocks observed by ISEE-3, in *Solar Wind Five*, edited by M. Neugebauer, *NASA Conf. Publ.*, *CP- 2280*, 711, 1983.

D. Berdichevsky, L-3 Communications, EER Systems, Inc., Largo, MD 20774, USA. (xrdbb@lepvx3.gsfc.nasa.gov)

L. Burlaga, N. Gopalswamy, and R. Lepping, Laboratory for Extra-terrestrial Physics, NASA Goddard Space Flight Center, Greenbelt, MD 20771, USA. (leonard.f.burlaga@nasa.gov; n_gopalswamy@yahoo.com; rpl@leprpl1.gsfc.nasa.gov)

T. Zurbuchen, Space Research Laboratory, University of Michigan, Ann Arbor, MI 48109, USA. (thomasz@umich.edu)